Increasing foot clearance in biped walking: Independence of body vibration amplitude from foot clearance

Hamid Reza Moballegh[1], Mojgan Mohajer[1], and Raul Rojas[1]

[1] Institut Für Informatik, FU-Berlin Takustr. 9 D-14195 Berlin, Germany
moballegh@gmail.com, mohajer@inf.fu-berlin.de, rojas@inf.fu-berlin.de

Abstract. A method of foot clearance achievement and frontal plane stability of 3D bipeds is mathematically analyzed. The independency of the robot's body vibration amplitude from the foot clearance is also proven. The analyzed method takes advantage of the sideways vibration of the body generated by periodically shortening each leg to obtain the required foot clearance. A mathematical model of the biped in the frontal plane is suggested and analyzed in two separate phases, resulted in the calculation of the steady state working point. It is demonstrated that in steady state, the amplitude of the body vibration becomes independent from the leg length vibration amplitude. A direct advantage of the proof is the possibility of achieving of high foot-to-ground distances by increasing the leg length vibration amplitude as the robot reaches its steady state. The results have been verified using both simulations and real robot experiments. To guarantee the stability of the robot in the transient phases a method is suggested based on an energy criterion.

1 Introduction

Stability and efficiency are two main aspects in today's walking humanoid research. There are known successful robots with high stability but poor performance [1]. Since they usually try to ignore the natural properties of the biped's body and urge predefined trajectories using powerful and exact servomotors. On the other hand there are several works poorly based on the mechanical properties of the biped which has been categorized under "passive Dynamic Walking" [1–5]. These approaches usually try to minimize or even avoid the existence of actuators. These solutions present almost human efficient robots, however they suffer from very limited stability. As reported in many of the published results, foot clearance is one of the key features in successful walking [7]. In some simulated 2D passive dynamic walking approaches any premature ground contact known as foot scuffing is easily ignored [2, 5]. Some others have tried to make special test grounds which allow the flying foot to continue flying even if it goes below the ground surface [3, 6]. Adding knees or using telescopic feet can be useful in a great extent [4, 7], but synchronization of the foot clearance mechanism with the walking gait needs special solutions. In addition, in 3D form, side stability

of the robot becomes a critical problem as the foot clearance increases. Some presented solutions to this problem are [8, 10, 11].

In servoed walking one of the common solutions is to transfer the COM projection, or more generally the ZMP to the stance foot support area before lifting the flying foot [9]. However the calculation of these parameters and proper reaction times need exact and reliable feedback data and control from the servos which cannot be expected from commercially available low-cost products.

One of the foot clearance achievement methods is to excite the foot lifting mechanism in sequence with a harmonic function which results in the side vibration of the body. This method has been commonly used in RoboCup humanoid league, however a theoretical analysis of its behavior is still missing. Towards this goal, a mathematical model of the biped in the frontal plane is suggested in section 2. The model is analyzed in two phases called "Flying" and "Heel Strike" phases. The steady state working point of the robot is calculated as the result of intersection between two functions extracted from the analysis of the phases. It is then shown that the steady state working point is independent from foot clearance. In section 3 the simulated results of the model are presented and the divergence of the method is demonstrated. In addition a method is suggested to stabilize the transient state of the robot and finally, experimental results are discussed in section 4.

2 Modeling the Biped in Frontal Plane

Fig. 1a shows the mathematical model used in this paper. The Model is similar to the 2D point foot walker described in [2] however it describes the behavior of the biped in the frontal plane instead of the sagittal plane. The whole mass of the model m is assumed to be placed at the hip joint. Leg opening angle α stands for the distance between the feet contact points and remains constant. The flying leg is shortened to l_f for the period of T seconds, while the stance leg has the maximum length l_s. The role of the legs will be exchanged as the period is elapsed.

The model is analyzed in two phases: The flying phase and the heel strike phase. In the flying phase, the model can be considered as an inverted pendulum hinged to the contact point of the stance foot to the ground. The flying phase starts with an initial angle β_0 equal to $\frac{\pi-\alpha}{2}$ (see Fig 1a). The initial speed is normally positive, so that the stance angle β starts to increase. The center of mass decelerates and stops after a while if (and it is normally the case) it does not have enough energy to reach the vertical position. The center of mass flies back again until the period is elapsed. The stance angle at this moment is called β_{hs}.

In the heel strike phase, the flying foot is re-extended to its original length and the stance foot is shortened. This usually leads to an impact between the flying foot and the ground surface, which can be simplified and modeled in two components of gaining and loosing energy. This simplification is possible since it can be shown that in steady state β_{hs} is very near to $\frac{\pi-\alpha}{2}$. Considering the

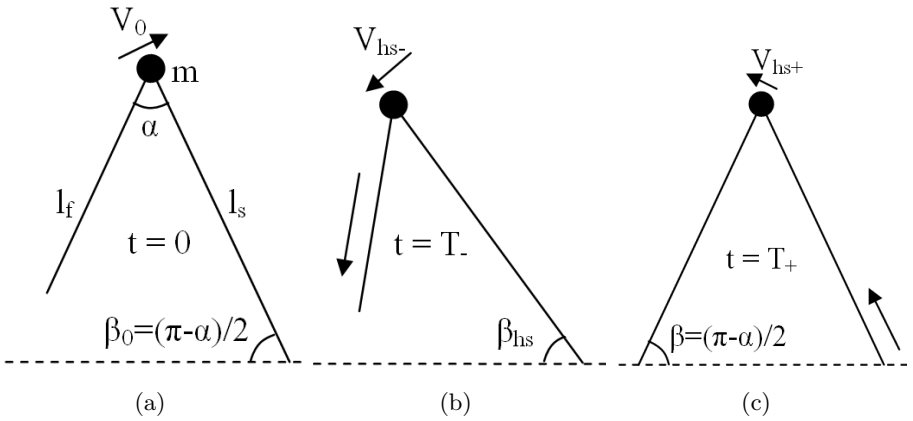

Fig. 1: Biped model (a) in initial conditions of the flying phase. (b) before heel strike and (c) after heel strike.

inelastic impact between the heel and the ground surface, there is a loss of kinetic energy caused by the sudden change of velocity vector of the center of mass. On the other hand it gains potential energy due to the lifting of its center of mass.

2.1 Analysis of the flying phase

Fig.2 shows the biped in the flying phase. As mentioned, the biped acts as an inverted pendulum in this phase. The tangent component of the weight is the only accelerating force applied to the model. Equation 1 describes the motion in this phase.

$$\ddot{\beta} = \frac{g \cos \beta}{l} \tag{1}$$

where:

$$\beta_0 = \frac{\pi - \alpha}{2}, \quad v_0 = v$$

The goal of analyzing the flying phase is to determine the value of β_{hs} as a function of the energy of the robot. The energy of the biped is a proper parameter showing the initial condition of the robot. As it remains constant during the flight, it can also be used in the analysis of the heel strike. The time of the flight is constant and equal to the period of the leg length vibrations. To solve the differential equation the normal numerical integration method over the period T is used. Fig.3a shows the simulation of several flying phases with different initial energies. In Fig.3b β_{hs} is presented as a function of the energy of the model. Following values has been given to the fixed variables used in the calculations

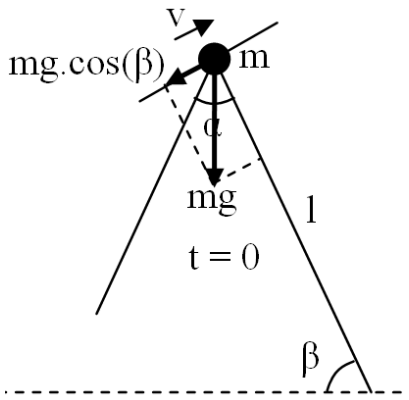

Fig. 2: Biped model in the flying phase

through out the paper:

$$m = 1\ Kg,\ \ l = 0.2\ m,\ \ T = 0.1\ s,\ \ \alpha = \frac{\pi}{4}\ rad$$

2.2 Analysis of the heel strike phase

In Fig.1b and Fig.1c the model is shown just before and after the heel strike. The changes in energy level of the model in the heel strike phase as discussed above can be considered separately over the kinetic and potential components of the energy of the biped. Equation 2 presents the energy of the model in terms of kinetic and potential energies in initial state.

$$E = mgl\cos\frac{\alpha}{2} + \frac{1}{2}mv_0^2 \tag{2}$$

As the period time T is elapsed the height of the center of mass is reduced to $l\sin(\beta_{hs})$. This difference in the potential energy is converted into kinetic energy. The whole energy of the biped can be presented with equation 3:

$$E = E_{hs-} = mgl\sin\beta_{hs} + mgl(\cos\frac{\alpha}{2} - \sin\beta_{hs}) + \frac{1}{2}mv_0^2 \tag{3}$$

The first term indicates the potential energy and the second and the third one show the kinetic energy of the system. Upon the occurrence of the heel strike, the potential energy of the COM will be increased to $mgl\cos(\frac{\alpha}{2})$. On the other hand, due to substitution of the stand point only the tangent component

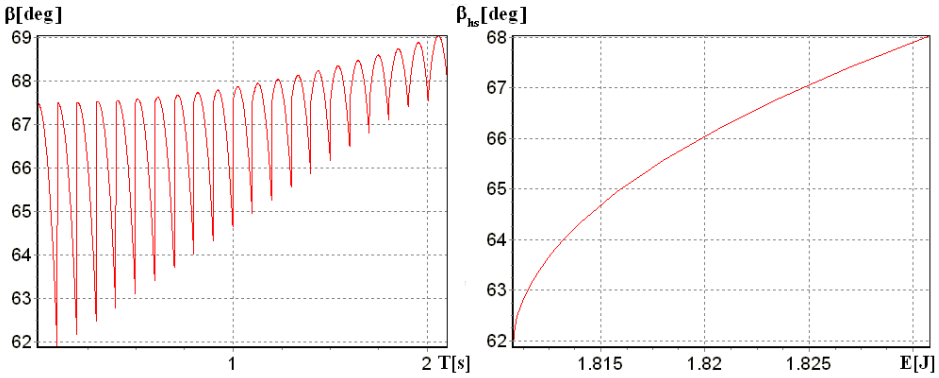

Fig. 3: Left: Simulation of several flying phases with increasing initial energies. Right: β_{hs} as a function of the energy of the model. Angles are presented in degrees to increase the readability.

of the velocity vector remains unchanged, and the centrifugal component will be eliminated due to the inelastic impact. The new energy can be shown as in equation 4:

$$E_{hs+} = mgl\cos\frac{\alpha}{2} + (mgl(\cos\frac{\alpha}{2} - \sin\beta_{hs}) + \frac{1}{2}mv_0^2)\cos^2\alpha \tag{4}$$

Equation 4 can be simplified and rephrased in terms of E:

$$E_{hs+} = mgl\cos\frac{\alpha}{2} + (E - mgl\sin\beta_{hs})\cos^2\alpha \tag{5}$$

The next step is to apply the steady state conditions to the model. In steady state, the energy of the biped should remain unchanged. This can be shown as:

$$E_{hs+} = E_{hs-} = E \tag{6}$$

By substituting equation 7 in equation 6, the steady state energy of the biped can be presented as the following function of the heel strike stance angle.

$$E(\beta_{hs}) = \frac{mgl\cos\frac{\alpha}{2} - (mgl\sin\beta_{hs})\cos^2\alpha}{\sin^2\alpha} \tag{7}$$

The function is shown in Fig.4 together with the numerical solution of the equation 1. The intersection point between these two functions determines the steady state working point. As it is observed, the length of the flying leg has no

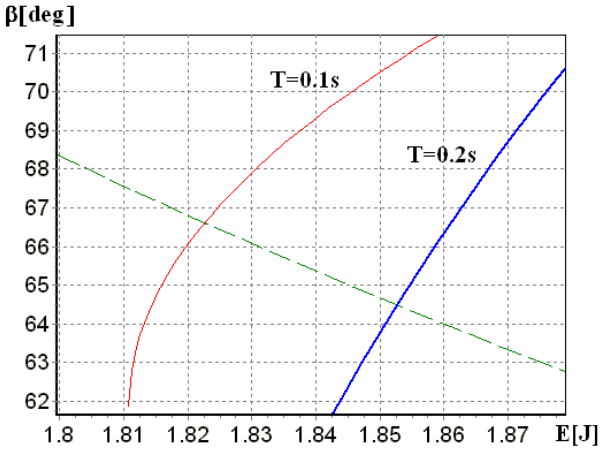

Fig. 4: Steady state condition relating E to β_{hs} (dashed) intersected with the function extracted in section 2.1 (solid) for two different values of T.

effect on the steady state working point. However, it will be further shown that this value is subject to a certain maximum. It means that the body vibration amplitude becomes independent from the foot clearance as the foot clearance exceeds a certain minimum.

2.3 Delayed and Premature Heel Strike

When the initial velocity of the center of mass exceeds a certain value, the stance angle remains still higher than $\frac{\pi-\alpha}{2}$ at the end of the flying phase. The result is that the re-extended leg does not reach the ground level at the time of T. The heel strike is called to be delayed in this case. A delayed heel strike has only the energy loss component and therefore cannot occur in steady state. It is however a useful event in transient state, as it reduces the energy of the biped and stabilizes the process. An early heel strike can also happen in which the biped lands on its shortened flying foot due to the lack of energy. A premature heel strike is the only event in which the length of the flying foot plays a role. Actually, the length of the flying foot limits the minimum stance foot angle. As observed in Fig.4, the less the stance foot angle becomes the higher amount of energy will be pumped in the system by the next heel strike. Therefore this parameter can be used to limit the energy of the biped to avoid instabilities as the biped goes through its transient condition. This method will be discussed further in the paper.

3 Simulation of the Biped Model

In order to test the convergence of the method and to compare the steady state working point with the one calculated in the previous analysis, the flying and the heel strike phases are simulated. The results are shown in Fig.5 and Fig.6 using two different leg opening angles. Other parameters remain unchanged. The model reaches its steady state after a few cycles of vibration and the steady state working point in both cases matches the values calculated in analysis.

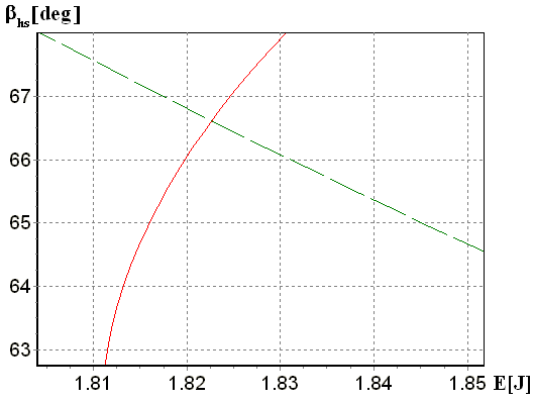

(a) calculated working point for $\alpha = \frac{\pi}{4}$

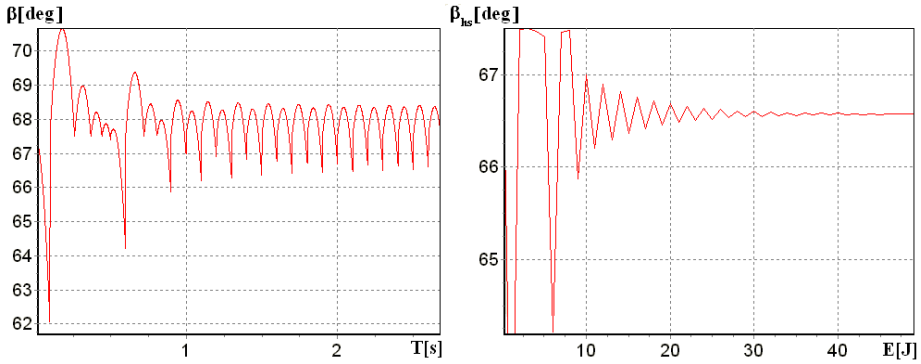

(b) stance angle (left) and heel strike stance angle (right)

Fig. 5: Simulation results: the model converges to the calculated steady state working point.

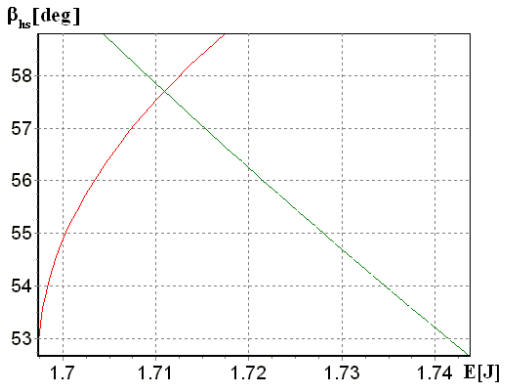

(a) calculated working point for $\alpha = \frac{\pi}{3}$

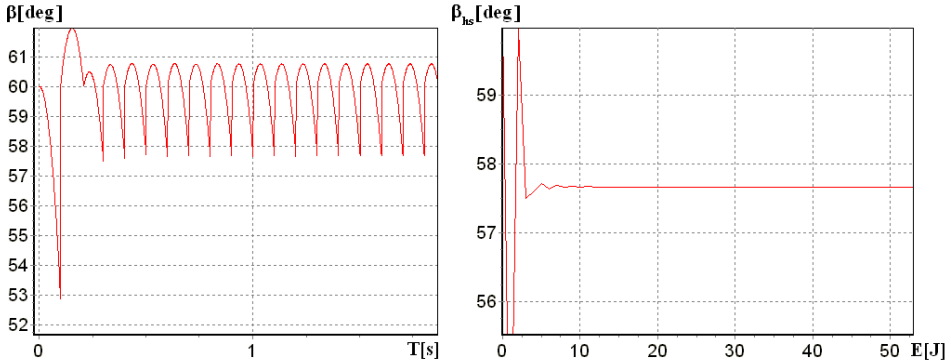

(b) stance angle (left) and heel strike stance angle (right)

Fig. 6: Simulation results: the model converges to the calculated steady state working point.

3.1 Stabilization of the Robot in Transient State

As observed so far, the biped model seems to have an internal feedback loop which regulates the energy. If the biped has too much energy it takes longer for it to fly back and therefore the stance angle of the heel strike becomes larger which means fewer energy for the next flight and vice versa. However this internal feedback loop can also make the system diverge under certain circumstances. To avoid this, the amount of energy pumped in the system should be limited before the system reaches its steady state and also when it leaves the steady state under any disturbances. The peak-to-peak value of the stance angle can be used as a suitable indicator of the energy of the robot. It is then enough to calculate this value in each period and assign a proportion of it to the foot clearance. The value

can also be low pass filtered to avoid rush changes of it. Applying this method in simulations shows a remarkable improvement in the convergence time and stability of the biped.

4 Experimental Results

The idea of increasing the foot clearance after the biped reaches the steady state has been successfully applied to the humanoid robot "LOLOS" which is going to attend RoboCup 2008 competitions. LOLOS is a 60 cm humanoid with 18 degrees of freedom. Our robot uses an implementation of the introduced method together with a modified version of passive dynamic walking. To be able to measure the stance angle of the robot, the stiffness of the servo motors belonging to the frontal plane movement of the feet is reduced to minimum. This gives the possibility to the robot to act more similar to the point foot model. The stance foot area remains on the ground surface during the flying phase. The peak-to-peak value used in the stabilization method discussed in 3.1 can be therefore extracted directly from the side servos. Fig.7 shows the angle value of the side servos of the robot together with its knee servos as an indicator of foot clearance, starting from initial rest condition until it reaches steady state. The independency of the side vibration amplitude from the foot clearance is observed clearly in the figure. Vibration amplitude remains almost constant as foot clearance increase during the first five seconds.

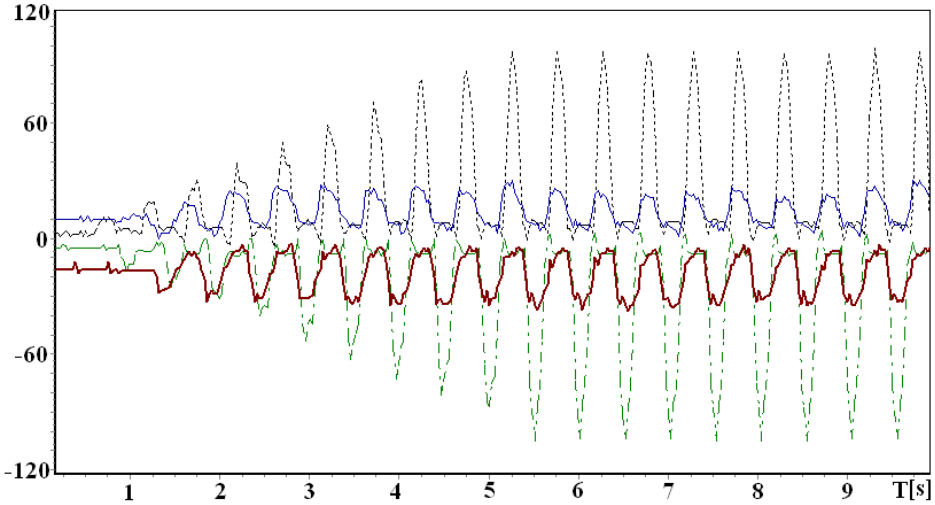

Fig. 7: Test results with the robot: The angle measurement of the side servos (solid) together with knee servos as an indicator of foot clearance (dashed).

5 Conclusion

We have theoretically analyzed the toddle like foot clearance achievement method and demonstrated that side stability in this method is independent from foot clearance. Hence, it is possible to achieve high foot-to-ground distances by increasing the leg length vibration amplitude as the robot reaches it steady state. We have examined this idea using simulations and real robot experiments. The experiment platform has been able to reach a maximum speed of 50 cm/s while no foot scuffing has been observed. The results show the success of the method.

References

1. S. Collins, A. Ruina, R. Tedrake, and M. Wisse: Efficient bipedal robots based on passive-dynamic walkers. Science, **307** (2005) 1082–1085
2. M. Garcia and A. Chatterjee and A. Ruina and M. Coleman: The simplest walking model: Stability, complexity, and scaling. Journal of Biomechanical Engineering - Transactions of the ASME, **120(2)** Apr(1998) 281–288
3. Tad McGeer.: Passive dynamic walking. International Journal of Robotics Research, (9(2)) April 1990 62–82
4. Tad McGeer.: Passive walking with knees. IEEE International Conference on Robotics and Automation (ICRA), **33** (1990) 1640–1645
5. Ambarish Goswami and Benoit Thuilot and Bernard Espiau: Compass-Like Biped Robot Part I : Stability and Bifurcation of Passive Gaits. Technical Report, INRIA, **RR-2996** October (1996)
6. F. Asano, M. Yamakita, K. Furuta,: Virtual passive dynamic walking and energy-based control laws. Intelligent Robots and Systems, (IROS 2000). Proceedings. 2000 IEEE/RSJ International Conference on **vol.2** (2000) 1149 - 1154
7. S. H. Collins, M. Wisse, and A. Ruina. : A Three-Dimensional Passive-Dynamic Walking Robot with Two Legs and Knees. International Journal of Robotics Research, **20(2)** (2001) 607–615
8. M. Wisse and A. L. Schwab: Skateboards, Bicycles, and Three-dimensional Biped Walking Machines: Velocity-dependent Stability by Means of Lean-to-yaw Coupling International Journal of Robotics Research, **24(6)** (2005) 417–429
9. S. Kajita, F. Kanehiro, K. Kaneko, K. Fujiwara, K. Harada, K. Yokoi, H. Hirukawa: Biped walking pattern generation by using preview control of zero-moment point Robotics and Automation, Proceedings. ICRA apos;03. IEEE International Conference on, **14-19(2)** Sept. (2003) 1620–1626
10. R. Tedrake, T.W. Zhang, Ming-fai Fong, H.S. Seung: Actuating a simple 3D passive dynamic walker Robotics and Automation, Proceedings. ICRA apos;04. IEEE International Conference on, **26(5)** (2004) 4656 - 4661
11. J. Donelan, D. Shipman, R. Kram, A. Kuo: Mechanical and metabolic requirements for active lateral stabilization in human walking Journal of Biomechanics, **6(37)** (2004) 827-835